Structural and Multidisciplinary Optimization (2018) 58:641–655
https://doi.org/10.1007/s00158-018-1915-5

RESEARCH PAPER

On the influence of local and global stress constraint and filtering radius on the design of hinge-free compliant mechanisms

Alexandre de Assis Pereira[1] · **Eduardo Lenz Cardoso**[1]

Received: 9 October 2017 / Revised: 12 January 2018 / Accepted: 17 January 2018 / Published online: 3 February 2018

Abstract
Distributed compliant mechanisms are components that use elastic strain to obtain a desired kinematic behavior. Compliant mechanisms obtained via topology optimization using the standard approach of minimizing/maximizing the output displacement with a spring at the output port, representing the stiffness of the external medium, usually contain one-node connected hinges. Those hinges are undesired since an ideal compliant mechanism should be a continuous part. This work compares the use of two strategies for stress constrained problems: local and global stress constraints, and analyses their influence in eliminating the one-node connected hinges. Also, the influence of spatial filtering in eliminating the hinges is studied. An Augmented Lagrangian formulation is used to couple the objective function and constraints, and the resulting optimization problem is solved by using an algorithm based on the classical optimality criteria approach. Two compliant mechanisms problems are studied by varying the stress limit and filtering radius. It is observed that a proper combination of filtering radius and stress limit can eliminate one-node connected hinges.

Keywords Compliant mechanisms · Topology optimization · Hinges · Stress constraint · Filter

1 Introduction

Compliant mechanisms are mechanical components formed by one or more parts, using elastic strain to obtain a desired kinematic behaviour (Lau et al. 2001). According to Midha et al. (1994), there are two main categories of compliant mechanisms: partially compliant mechanisms, consisting of rigid links and flexible parts, and fully compliant mechanisms, composed by flexible members or joints. Fully compliant mechanisms can be further classified in two categories: lumped and distributed compliant mechanisms. In lumped compliant mechanisms, the flexibility is provided in localized areas, and in distributed compliant mechanisms, the compliance is distributed through most of the mechanism.

An effective way to design compliant mechanisms is through a topology optimization problem. Topology optimization addresses the optimal distribution of one or more materials within a prescribed design domain in order to obtain the best structural performance respecting the design requirements (Sigmund and Maute 2013). The design variables of a topology optimization problem, known as densities or relative densities (in order to not be confused with the usual material density), are associated to the effective material properties of each point of the design domain.

A common approach to address the optimal design of compliant mechanisms is proposed by Sigmund (1997), where a spring is used to represent the stiffness of the external medium. The objective is to minimize/maximize the output displacement exerted on this spring, with some displacement constraints to enforce the kinematic behavior. Despite its apparent simplicity, this approach is broadly used since it is very general and can be easily extended to multi-physics and non-linear problems (Liu et al. 2017).

Nevertheless, this formulation, as well as other similar approaches, have the undesirable tendency to introduce one-node connected hinges into the final topology, as depicted in Fig. 1. As discussed in Cardoso and Fonseca (2004) and Yin and Ananthasuresh (2003), the appearance of one-node connected hinges can be seen as a model problem, since the maximization of the output displacement conflicts

✉ Eduardo Lenz Cardoso
eduardo.cardoso@udesc.br

[1] Mechanical Engineering Department, State University of Santa Catarina, Joinville, SC 89.219-710, Brazil

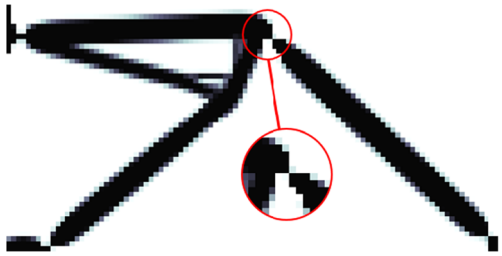

Fig. 1 One-node hinge in a symmetric analysis of an inverter mechanism

with the storage of strain energy expected in structures with distributed compliance. Thus, the optimizer uses the artifice of (almost) rigid links connected by one-node connections, taking advantage of the lack of rotational stiffness in the traditional elasticity equations. Also, Wang et al. (2011) show that this effect is so prominent that even the Heaviside filter alone is not sufficient to hinder its appearance.

Thus, the use of simple filtering cannot fix this shortcoming in the traditional approach to design of compliant mechanisms using topology optimization. In order to circumvent this problem, many authors proposed alternate formulations, use of alternate material parametrizations, addition of physical constraints, addition of geometric constraints and the consideration of uncertainties, to name a few.

One of the first proposals for circumventing one-node connected hinges as well as checkerboards was proposed by Poulsen (2002). In this geometric approach, a global constraint associated to the pattern of black and white elements around the one-node connected hinge is imposed. This simple and elegant solution avoids the appearance of hinges, but those are transformed in very thin reinforcements as the mesh is refined, since this approach is not mesh-independent. Wang and Zhang (2012) also address the design of hinge-free compliant mechanisms using an optimization problem based on pairs of curves and solved by a genetic algorithm. Saxena and Mankame (2007) use hexagonal cells for domain discretization, ensuring edge-connectivity between subregions throughout the domain and thus circumventing the hinges. The use of multiresolution in the framework of isogeometric analysis applied to topology optimization is proposed by Lieu and Lee (2017), where a single example of an inverter mechanism with no hinges is presented.

Many works also use the level set method applied to design hinge-free mechanisms through shape and topology optimization, like Luo et al. (2008) and Zhu et al. (2013). Xia and Shi (2016) propose a multi-objective optimization problem, where the compliance of two additional load cases are considered alongside the displacement at the output port. A similar approach is proposed by Li and Zhu (2016), also using the level set method and by Zhu et al. (2014), using the traditional SIMP parametrization.

In the realm of alternate formulations, Cardoso and Fonseca (2004) propose the maximization of a measure of the strain energy stored in solid elements. The kinematic behavior of the compliant mechanisms is prescribed by a set of displacement constraints for both the input and output ports. The obtained topologies are free from hinges, but this formulation is not as direct as the traditional formulation. Mechanisms with distributed compliance were also achieved by Yin and Ananthasuresh (2003), where two formulations are discussed: one based in the distortional energy of a given patch around each element and one based in the relative rotation between diagonals around each node. Lee and Gea (2014), propose the use of a strain based topology optimization method, reducing localized high strain in compliant joints, thus hindering the appearance of hinges.

Sigmund (2009) and Lazarov et al. (2011) propose the use of both *erode* and *dilate* operators to simulate the uncertainties associated to the fabrication of compliant mechanisms, as a worst case design problem. The results have no hinges and no gray regions. This formulation is further enhanced by Lazarov et al. (2012) where the geometrical uncertainties are modeled using a stochastic field. The results are also free of hinges. Kogiso et al. (2008) consider uncertainties in applied loads to design compliant mechanisms, by means of mutual compliances. For the data case presented, it seems that the formulation does not eliminates hinges. Chen et al. (2010) use level set with consideration of random field uncertainty in loading and material properties. This is one of the few works addressing 3D results as well. The results presented in this reference are hinge-free and robust. Maute and Frangopol (2003) also consider uncertainties in both material parameters, loading and boundary conditions. The results show the importance of considering uncertainties in topology optimization, although the topologies contain hinges.

The use of filtering to avoid the appearance of hinges is also discussed in the literature. As already mentioned, Wang et al. (2011) show that the use of the traditional Heaviside filter is not sufficient to prevent hinges. Enhanced approaches are also presented in the literature, as for example, Zhou et al. (2015) propose the use of geometric constraints in a filtering-threshold topology optimization (three-field scheme). The results are hinge-free. Li and Khandelwal (2015b) discuss the use and performance of continuation methods and volume preserving filtering and the results, besides eliminating one-node connetions, present very thin regions. Li and Khandelwal (2015a) also propose the consideration of microstructural effects, indicating an important effect on optimal designs. Some of the results are hinge-free. Carstensen and Guest (2013)

discuss the use of two-phase projection filters and the results contains thin connections instead of one-node connected elements.

A natural approach to the design of hinge-free distributed compliant mechanisms is the consideration of stress constraints. This physical set of constraints should, ideally, avoid the appearance of one-node connections. Lopes and Novotny (2016) study the use of the Topological Derivative to enforce stress constraints in the design of compliant mechanisms. The stress constraint is expressed as a set of von Mises stress penalty functions and the hinges are replaced by thin compliant connections. A global stress constraint is used in de Leon et al. (2015) in order to alleviate one-node hinges, also resulting in very thin compliant regions replacing the hinges. Thus, the simple use of stress constraints alone does not solve the problem.

Those results indicate that, in order to obtain hinge-free geometries, the use of stress constraints plus high order elements and fine meshes could be applied at the optimization problem, but it would be computationally inefficient and may not eliminate the solid hinges entirely (Sigmund 2007). Also, the use of global stress constraints seems to result in thin reinforcements, indicating the use of localized flexibility and thus a lumped distributed compliant mechanism. In regards to filtering, the results found in the literature suggest that the use of simple filtering techniques alone cannot avoid the appearance of hinges.

Thus, the main objective of this work is to study the joint use of local stress constraints and proper filter radius to design distributed compliant mechanisms. Also, the performance of both local and global stress constraints are compared and discussed. To this end, both formulations are written as an Augmented Lagrangian formulation and solved by using the traditional first order optimality criteria proposed by Bendsøe and Kikuchi (1988). The material parametrization used for the design of compliant mechanisms is the traditional SIMP (*Solid Isotropic Material with Penalization*) and the effective stress tensor is parametrized using the qp approach (Bruggi 2008). The filter used in this study is the traditional spatial neighborhood density filtering method applied directly to the relative density (as summarized by Sigmund (2007)).

2 Stress evaluation

The topology optimization with stress constraint formulation is highly nonlinear with respect to the design variables, and faces some difficulties (Yang and Chen 1996). The first difficulty is related to the fact that stress is a local measure, leading to a large number of constraints. Second, due to the material parameterization, the solution space is irregular (singularity problem) (Bruggi 2008).

The singularity problem appears due to the fact that the use of a consistent material parametrization makes the stress independent of the relative densities (Duysinx and Bendsøe 1998). In order to smooth the feasible design space some relaxation methods were developed, such as ϵ*-relaxation* (Cheng and Guo 1997) and *qp-relaxation* methods (Bruggi 2008). At *qp-relaxation* the effective stress tensor at the superconvergent point k of an element e can be defined by

$$\boldsymbol{\sigma}_{e,k} = \rho_e^{p-q}\boldsymbol{\sigma}_{e,k}^0 \quad p > q, \tag{1}$$

where ρ_e is the relative density of element e, p and q are respectively the SIMP penalization and the stress relaxation parameter and $\boldsymbol{\sigma}_{e,k}^0$ is the stress tensor evaluated by considering the base material. The exponent $p - q$ operates on elements with intermediate relative density, since the elements with relative density equals to 1 have their original constitutive tensor unmodified, as well as happens with SIMP. Actually, q must be equal to p, but this would not relax the solution space (Duysinx and Bendsøe 1998). Values $p > q$ give no discontinuity of the stress measure at elements with relative density close to zero, thus relaxing the design space.

As the stress is a local measure, an optimization problem with stress constraints can have a high number of nonlinear constraints. Thus, a common approach presented in the literature is to transform the large number of stress constraints in a single one or in few groups. Those constraints are known as global constraints (Yang and Chen 1996; Le et al. 2010; Holmberg et al. 2013). A global stress constraint using the P-norm is written as

$$\|\boldsymbol{\sigma}_{eq}\|_P \leq \bar{\sigma}, \tag{2}$$

where $\boldsymbol{\sigma}_{eq}$ is a vector containing the equivalent stresses in all the superconvergent points of the mesh. For $P \to \infty$, $\|\boldsymbol{\sigma}_{eq}\|_P \to max(\boldsymbol{\sigma}_{eq})$. Since the use of large values of P lead to numerical problems and prevents the use of gradient based methods, Le et al. (2010) propose the use of

$$c^i\|\boldsymbol{\sigma}_{eq}\|_P \leq \bar{\sigma}, \tag{3}$$

with

$$c^i = \frac{\max\left(\boldsymbol{\sigma}_{eq}^{i-1}\right)}{\|\boldsymbol{\sigma}_{eq}^{i-1}\|_P}, \tag{4}$$

where $\max\left(\boldsymbol{\sigma}_{eq}^{i-1}\right)$ is the maximum equivalent stress of the previous iteration. Thus, as the number of iterations increases, the ratio between the actual norm to the previous norm tends to one, such that the global constraint can be read as $\max\left(\boldsymbol{\sigma}_{eq}^{i-1}\right) \leq \bar{\sigma}$. Other approach to include a global measure is the use of aggregation formulations, such as the K–S function, for example (Luo et al. 2013; Oest and Lund 2017).

Another approach is to independently consider all the stress constraints. This can be implemented by the selection of a set of active constraints, as in Duysinx and Bendsøe (1998), where the local stress constraints are replaced by one or several integrated stress criteria. However the disadvantage is that it is difficult to find a general procedure able to control efficiently the local peak values. Other authors effectively consider all the stress constraints by using the Augmented Lagrangian technique, (Fancello 2006; Emmendoerfer and Fancello 2014; da Silva and Cardoso 2017). This approach is discussed in the following section.

To better represent the bending behavior and also to better evaluate the stress, a nonconforming finite element is used in this work. The formulation is based in Pian and Wu (2005), where the traditional four node bilinear isoparametric element is modified by the inclusion of two additional "bubble" or incompatible functions, associated to new degrees of freedom $\boldsymbol{\alpha}$. The element is then condensed to an equivalent four-node element with the same number of degrees of freedom of the traditional bilinear finite element.

Of special interest to the forthcoming equations is the matrix $\mathbf{A}$, mapping the local 8 degrees of freedom of an element to a 12×1 vector containing the usual degrees of freedom plus 4 additional incompatible degrees of freedom. Thus, considering the the qp parameterization and the inclusion of the incompatible functions, the effective stress tensor at the superconvergent point k of an element e can be re-written as

$$\boldsymbol{\sigma}_{e,k} = \rho_e^{p-q} \mathbf{D}_e^0 \mathbf{B}_{e,k} \mathbf{A}_e \mathbf{q}_e, \tag{5}$$

where $\mathbf{D}_e^0$ is the original constitutive tensor of element e, $\mathbf{B}_{e,k}$ contains the derivative of the traditional plus the incompatible interpolation functions at k and $\mathbf{q}_e$ is the nodal displacement vector of the element e. This formulation has the additional benefit that this element has 4 superconvergent stress points ($k = 1..4$).

Note that by using an homogeneous mesh where all elements are equal, $\mathbf{D}_e^0$, $\mathbf{B}_{e,k}$ and $\mathbf{A}_e$ have the same value for all elements, such that (5) becomes

$$\boldsymbol{\sigma}_{e,k} = \rho_e^{p-q} \mathbf{D}^0 \mathbf{B}_k \mathbf{A} \mathbf{q}_e. \tag{6}$$

The equivalent *von Mises* stress is written as

$$\sigma_{eq_{e,k}} = (\boldsymbol{\sigma}_{e,k}^T \mathbf{M} \boldsymbol{\sigma}_{e,k})^{1/2}, \tag{7}$$

where

$$\mathbf{M} = \begin{bmatrix} 1 & -1/2 & 0 \\ -1/2 & 1 & 0 \\ 0 & 0 & 3 \end{bmatrix}, \tag{8}$$

for plane stress problems.

3 Optimization strategy

Considering that stress is a local quantity, a large number of constraints must be considered in the optimization problem, leading to a large computational cost (da Silva and Cardoso 2017). Such large number of constraints greatly reduces the effectiveness of many popular optimizers. Thus, a suggested procedure is the use of the Augmented Lagrangian formulation, which can easily deal with a large number of constraints without being computational expensive (Emmendoerfer and Fancello 2014; da Silva and Cardoso 2017). For the application of the Augmented Lagrangian formulation, consider the generic topology optimization problem with volume constraint

$$\begin{aligned} &Min/Max \quad f(\boldsymbol{\rho}) \\ &S.t \\ &\qquad g_k(\boldsymbol{\rho}) \le \bar{g}_k \;\; k = 1..Ng \\ &\qquad V \le \bar{V} \qquad\qquad , \\ &\qquad 0 < \rho_e \le 1 \;\; e = 1..N_e \end{aligned} \tag{9}$$

where $f(\boldsymbol{\rho})$ is the objective function, $g_k(\boldsymbol{\rho}) \le \bar{g}_k$ is an inequality constraint k, Ng is the number of inequality constraints, V is the volume of the optimized structure, $\bar{V}$ is the volume limit and N_e is the number of design variables (elements).

An alternative formulation for the optimization problem stated in (9) can be written as

$$\begin{aligned} &Min \;\; \mathcal{L}(\boldsymbol{\rho}, \boldsymbol{\mu}, r) = f(\boldsymbol{\rho}) + \tfrac{r}{2} \left\{ \sum_{k=1}^{Ng} \left\langle \tfrac{\mu_k}{r} + g_k(\boldsymbol{\rho}) - \bar{g}_k \right\rangle^2 \right\} \\ &S.t \\ &\qquad\qquad V \le \bar{V}, \\ &\qquad 0 < \rho_e \le 1 \quad e = 1..N_e \end{aligned} \tag{10}$$

where $\boldsymbol{\mu}$ are the Lagrange multipliers associated to the inequality constraints, r is a penalty parameter and $\langle a \rangle$ is defined as $\max(a, 0)$. Note that the objective function of (10) is the Augmented Lagrangian formulation of the optimization problem defined in (9) without the volume constraint.

A very important variable when using Augmented Lagrangian formulation is the penalty parameter r. Due to the magnitude of displacement and stress constraints, two separated penalizations may be adopted (one for each constraint type), if necessary. Defining the penalty parameters is not an easy task. For achieving consistent geometries, a good reference is to define the penalization value as

$$r = \frac{10 f(\boldsymbol{\rho})}{\sum_{k=1}^{Ng} \left\langle \frac{g_k(\boldsymbol{\rho})}{\bar{g}_k} - 1 \right\rangle}, \tag{11}$$

which was defined after tests using different conditions and resulted in a good proportion between objective function

and the constraint term of the Augmented Lagrangian formulation. Using an excessively large penalization will result in complex geometries due to bad local optima caused by high non-linearity. Very small penalization values make it hard to satisfy the constraints.

The Lagrange multipliers update for the next iteration of the external loop $(j+1)$ are defined by

$$\mu_k^{j+1} = \left\langle \mu_k^j + r^j \left(g_k(\boldsymbol{\rho}) - \bar{g}_k\right) \right\rangle, \tag{12}$$

and the penalty update in the external loop is

$$r^{j+1} = \gamma r^j, \ \gamma > 1. \tag{13}$$

The design variables are updated using the Optimality Criteria, as proposed in (Bendsøe and Sigmund 2004). Here, a Lagrangian function Q is formed by the Augmented Lagrangian function of the optimization problem $(\mathcal{L})$ and the volume constraint $\left(V - \bar{V}\right)$, resulting in

$$Q\left(\boldsymbol{\rho}, \psi\right) = \mathcal{L} + \psi \left(V - \bar{V}\right), \tag{14}$$

where ψ is the Karush-Kuhn-Tucker multiplier for the volume constraint.

The optimality criteria optimization algorithm, as explained in Bendsøe and Sigmund (2004), is used to obtain the optimal solution of the problem defined in (14). It should be stressed that the problem defined in (10) can be solved by using any appropriate optimization algorithm, but there is a good rationale the present choice: this method is known to work well with similar topology optimization problems, that is, a large number of bounded design variables and a single linear constraint. As it will be discussed in the result section, the performance of this optimization algorithm is highly dependent on the degree of non linearity of the problem, since it is based on the first order optimality conditions.

The traditional density filter, Bruns and Tortorelli (2001), is used in this work to study the influence of a simple filtering procedure in the elimination of the one-node connections when used with stress constraints. This method changes the definition of the design variables in order to approximately impose a minimum length scale to the desired topology. Using the traditional linear weights and centroidal distances, this change of variables can be defined as

$$\tilde{\rho}_i = \sum_{j \in Ne_i} \frac{w_{ji}\rho_j}{w_{ji}}, \tag{15}$$

where $\tilde{\rho}_i$ is the filtered relative density of central element i, Ne_i are the elements situated in the neighbourhood area of the central element (including i) and w_{ji} is a linear weight function,

$$w_{ij} = 1.0 - \frac{d_{ij}}{R}, \tag{16}$$

where d_{ij} is the centroidal distance between element i and element j and R is the filtering radius from the centroid of the central element.

The gradient computed with filtered relative density must be evaluated with respect to the original design variables as well. Thus, for a general function $\mathcal{L}$, the gradient can be corrected by

$$\frac{d\mathcal{L}}{d\rho_m} = \frac{d\mathcal{L}}{d\tilde{\rho}_i}\frac{d\tilde{\rho}_i}{d\rho_m}. \tag{17}$$

It is assumed throughout this text that the relative density are properly filtered and that all quantities and their sensitivities are evaluated with respect to these filtered variables. Also, it is assumed that the optimization problem is solved with respect to the design variables $\boldsymbol{\rho}$ and that all the sensitivities are properly converted, as shown in (17).

4 Compliant mechanisms design with local stress constraint

The local stress constraint is defined by

$$\sigma_{eq_{e,k}}(\boldsymbol{\rho}) \leq \bar{\sigma}, \tag{18}$$

where $\bar{\sigma}$ is the stress limit.

The classical approach for the design of compliant mechanism using topology optimization, (Sigmund 1997), consists on the minimization or maximization of a set of output displacements, while constraining a set of input displacements. Adding local stress constraints, the standard form of the optimization problem can be written as

$$\begin{array}{ll} Min & \sum_{i=1}^{N_{out}} U_{out_i} S_{out_i} \\ S.t & \\ & V \leq \bar{V} \\ & \left(U_{in_j} - \bar{U}_{in_j}\right) S_{in_j} \leq 0 \quad j = 1..N_{in} \\ & \sigma_{eq_{e,k}} - \bar{\sigma} \leq 0 \qquad e = 1..N_e, \ k = 1..4 \\ & 0 < \rho_i \leq 1, \qquad i = 1..N_e \end{array} \tag{19}$$

where N_{out} and N_{in} are the number of output and input displacements, U_{out} is the displacement in the output region, V is the volume, $\bar{V}$ is the volume limit established for the optimization problem, U_{in} is the input displacement, $\bar{U}_{in}$ is the input displacement limit, as shown in Fig. 2, Ne and k are respectively the number of element in the finite elements mesh and the number of superconvergent points at the element e and S_{out_i} and S_{in_j} are the displacement directions, such that

$$S_{out_i} = \begin{cases} 1 & \text{for minimization} \\ -1 & \text{for maximization} \end{cases}, \tag{20}$$

and

$$S_{in_j} = \begin{cases} 1 & \text{for } \leq \text{ constraint} \\ -1 & \text{for } \geq \text{ constraint} \end{cases}. \tag{21}$$

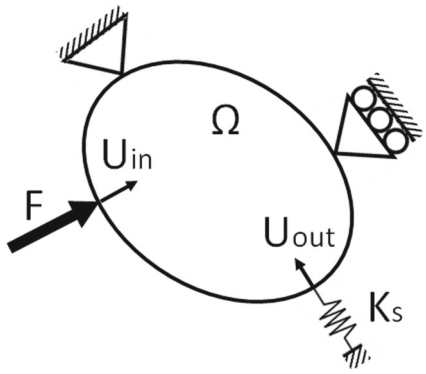

Fig. 2 Compliant mechanism design domain (adapted from (Sigmund 1997))

The Augmented Lagrangian formulation without the volume constraint is

$$\mathcal{L}(\boldsymbol{\rho},\boldsymbol{\phi},\boldsymbol{\mu},r_d,r_s)=\sum_{i=1}^{N_{out}} S_{out\,i}\mathbf{L}_{out\,i}^T\mathbf{U}+\frac{r_d}{2}\sum_{j=1}^{N_{in}}\left\langle\frac{\mu_j}{r_d}+\left(\frac{\mathbf{L}_{in\,j}^T\mathbf{U}}{\bar{U}_{in\,j}}-1\right)S_{in_j}\right\rangle^2 +\frac{r_s}{2}\sum_{e=1}^{N_e}\sum_{k=1}^{4}\left\langle\frac{\phi_{e,k}}{r_s}+\frac{\sigma_{eq_{e,k}}}{\bar{\sigma}}-1\right\rangle^2+\boldsymbol{\lambda}^T(\mathbf{KU}-\mathbf{F}), \tag{22}$$

where r_s and r_d are penalty parameters for stress and displacement constraints, $\boldsymbol{\phi}$ and $\boldsymbol{\mu}$ are Lagrange multipliers for stress and displacement constraints, $S_{out_i}\mathbf{L}_{out_i}^T\mathbf{U} = U_{out_i}S_{out_i}$ and $S_{in_i}\mathbf{L}_{in_i}^T\mathbf{U} = U_{in_i}S_{in_i}$. $\boldsymbol{\lambda}$ is the adjoint vector, $\mathbf{K}$ is the global stiffness matrix and $\mathbf{F}$ is a design independent force vector. There are two distinct penalty parameters in order to avoid numerical problems, since even if the constraints are normalized, the sums change the order of magnitude of each kind of constraint.

The gradient of the Augmented Lagrangian function, (22), with respect to a design variable ρ_m is

$$\frac{d\mathcal{L}}{d\rho_m}=r_s\sum_{k=1}^{4}\left[\left\langle\frac{\phi_{m,k}}{r_s}+\frac{\sigma_{eq_{m,k}}}{\bar{\sigma}}-1\right\rangle\frac{\sigma_{m,k}^T\mathbf{M}(p-q)\rho_m^{(p-q-1)}\mathbf{D}^0\mathbf{B}_k\mathbf{A}\mathbf{q}_m}{\sigma_{eq_{m,k}}\bar{\sigma}}\right] +\boldsymbol{\lambda}_m^T p\rho_m^{(p-1)}\mathbf{K}_m^0\mathbf{q}_m, \tag{23}$$

where the global adjoint vector $\boldsymbol{\lambda}$ is defined by

$$\mathbf{K}^T\boldsymbol{\lambda}=-\sum_{i=1}^{N_{out}} S_{out_i}\mathbf{L}_{out_i}-r_d\sum_{j=1}^{N_{in}}\left[\left\langle\frac{\mu_j}{r_d}+\left(\frac{U_{in_j}}{\bar{U}_{in_j}}-1\right)S_{in_j}\right\rangle\frac{\mathbf{L}_{in_j}S_{in_j}}{\bar{U}_{in_j}}\right] -r_s\sum_{e=1}^{N_e}\sum_{k=1}^{4}\left[\left\langle\frac{\phi_{e,k}}{r_s}+\frac{\sigma_{eq_{e,k}}}{\bar{\sigma}}-1\right\rangle\frac{\sigma_{e,k}^T\mathbf{M}\rho_e^{(p-q)}\mathbf{D}^0\mathbf{B}_k\mathbf{A}\mathbf{H}_e}{\sigma_{eq_{e,k}}\bar{\sigma}}\right]^T, \tag{24}$$

where $\mathbf{H}_e$ is a localization matrix such that $\mathbf{H}_e\mathbf{U}=\mathbf{q}_e$.

In the end of each external loop (n) the Lagrange multipliers are updated by

$$\mu_j^{(n+1)}=\left\langle\mu_j^{(n)}+r_d^{(n)}S_{in_j}\left(\frac{\mathbf{U}_{in_j}}{\bar{U}_{in_j}}-1\right)\right\rangle, \tag{25}$$

and

$$\phi_{e,k}^{(n+1)}=\left\langle\phi_{e,k}^{(n)}+r_s^{(n)}\left(\frac{\sigma_{eq_{e,k}}}{\bar{\sigma}}-1\right)\right\rangle, \tag{26}$$

and the penalties are updated by

$$r_d^{(n+1)}=\gamma_d r_d^{(n)}, \tag{27}$$

and

$$r_s^{(n+1)}=\gamma_s r_s^{(n)}, \tag{28}$$

where γ_d and γ_s are the penalty update factors.

5 Compliant mechanisms design with global stress constraint

The consideration of a global measure of stress constraint on the previous formulation is straightforward. Using (3), the optimization problem becomes

$$\begin{array}{ll} Min & \sum_{i=1}^{N_{out}} U_{out_i}S_{out_i} \\ S.t & \\ & V\le\bar{V} \\ & \left(U_{in_j}-\bar{U}_{in_j}\right)S_{in_j}\le 0\ \ j=1..N_{in}. \\ & c^i||\boldsymbol{\sigma}_{eq}||_P-\bar{\sigma}\le 0 \\ & \mathbf{0}<\boldsymbol{\rho}\le\mathbf{1} \end{array} \tag{29}$$

The Augmented Lagrangian formulation without the volume constraint is

$$\mathcal{L}(\boldsymbol{\rho},\boldsymbol{\phi},\boldsymbol{\mu},r_d,r_s)=\sum_{i=1}^{N_{out}} S_{out_i}\mathbf{L}_{out_i}^T\mathbf{U}+\frac{r_d}{2}\sum_{j=1}^{N_{in}}\left\langle\frac{\mu_j}{r_d}+\left(\frac{U_{in_j}}{\bar{U}_{in_j}}-1\right)S_{in_j}\right\rangle^2 +\frac{r_s}{2}\left\langle\frac{\phi_s}{r_s}+\frac{c^i||\boldsymbol{\sigma}_{eq}||_P}{\bar{\sigma}}-1\right\rangle^2+\boldsymbol{\lambda}^T(\mathbf{KU}-\mathbf{F}). \tag{30}$$

The gradient of the Augmented Lagrangian function with respect to a design variable ρ_m is

$$\frac{d\mathcal{L}}{d\rho_m}=r_s\left\langle\frac{\phi_s}{r_s}+\frac{c^i||\boldsymbol{\sigma}_{eq}||_P}{\bar{\sigma}}-1\right\rangle\frac{c^i}{\bar{\sigma}||\boldsymbol{\sigma}_{eq}||_P} \sum_{k=1}^{4}\left[\sigma_{eq_{m,k}}^{(P-2)}\boldsymbol{\sigma}_{m,k}^T\mathbf{M}(p-q)\rho_m^{(p-q-1)}\mathbf{D}^0\mathbf{B}_k\mathbf{A}\mathbf{q}_m\right]+\boldsymbol{\lambda}_m^T p\rho_m^{(p-1)}\mathbf{K}_m^0\mathbf{q}_m, \tag{31}$$

where the global adjoint vector $\boldsymbol{\lambda}$ is defined by

$$\mathbf{K}\boldsymbol{\lambda} = -\sum_{i=1}^{N_{out}} S_{out_i}\mathbf{L}_{out_i} - r_d \sum_{j=1}^{N_{in}} \left[\left\langle \frac{\mu_j}{r_d} + \left(\frac{U_{in_j}}{\bar{U}_{in_j}} - 1 \right) S_{in_j} \right\rangle \frac{\mathbf{L}_{in_j} S_{in_j}}{\bar{U}_{in_j}} \right]$$
$$-r_s \left\langle \frac{\phi_s}{r_s} + \frac{c^i ||\boldsymbol{\sigma}_{eq}||_P}{\bar{\sigma}} - 1 \right\rangle \frac{c^i}{\bar{\sigma}||\boldsymbol{\sigma}_{eq}||_P} \sum_{e=1}^{N_e} \sum_{k=1}^{4} \left[\sigma_{eq_{e,k}}^{(P-2)} \boldsymbol{\sigma}_{e,k}^T \mathbf{M} \rho_e^{(p-q)} \mathbf{D}^0 \mathbf{B}_k \mathbf{A} \mathbf{H}_e \right]. \quad (32)$$

In the end of each external loop (n) the Lagrange multipliers are updated by (25) and

$$\phi_s^{(n+1)} = \left\langle \phi_s^{(n)} + r_s^{(n)} \left(\frac{c^i ||\sigma_{\mathbf{eq}}||_P}{\bar{\sigma}} - 1 \right) \right\rangle, \quad (33)$$

and the penalties are updated according to (27) and (28).

6 Results

For better understanding the influence of local stress constraint, global stress constraint and filtering radius regarding one-node connected hinges, some studies were performed and the results are shown in this section. Two problems of compliant mechanisms designed by topology optimization are analyzed. Few works in the literature expose all necessary information to replicate the problems and very few of them use real material properties. So the studies were based on Cardoso and Fonseca (2004) and adapted to be applied in the presented formulation. The material is Nylon, with Young's modulus $E = 3\ GPa$ and Poisson's coefficient $\nu = 0.4$. A plane stress model is used and the thickness of the domain is 5 mm. The problems are symmetric, such that only half of the domains are considered.

The internal problem is solved by using Optimality Criteria, with tolerance of 1×10^{-10} and fixed moving limits of ±2%. This small moving limit is used in order to allow the comparison of two different problems in regards to the non linearity. As it will be shown, the global stress constraint is more non linear than the local stress approach. This can be explained by the fact that in the local approach just few constraints are active at the optimum, such that most multipliers are zero. On the other hand, the global approach is a P norm of a large number of stress points and it is always active. Numerical experiments performed for this research indicate that the optimality criteria can easily handle the local stress constraint even for larger values of moving limits, but this is not true for the global approach.

The number of external loops, 12, in the Augmented Lagrangian approach was defined according to tests performed in order to obtain well defined and stable topologies.

Other parameters are shown in Table 1. The exponent q has been set after tests aiming to achieve geometries without significant stress values in void regions.

The usual greyscale palette is used to represent both relative density and equivalent stress fields in this section. In relative density images, white represents the lower density and black the base material. In equivalent stress images, white represents low stress magnitudes, where black represent the larger values of equivalent stress.

Table 1 Parameters used in the optimization problems

Variable	Value	Description
E	3 GPa	Young's modulus
ν	0.4	Poisson's coefficient
F_{in}	200 N	Input force
K_{out}	1×10^5 N/m	Output spring stiffness
$\bar{U}_{in}$	2 mm	Input displacement limit
$\bar{V}$	25%	Volume fraction
p	3	SIMP penalization
q	1.5	Stress relaxation
γ	1.1	Penalization update factor

6.1 Inverter mechanism

Consider the design domain shown in Fig. 3. The input force and output spring are distributed along 5 mm

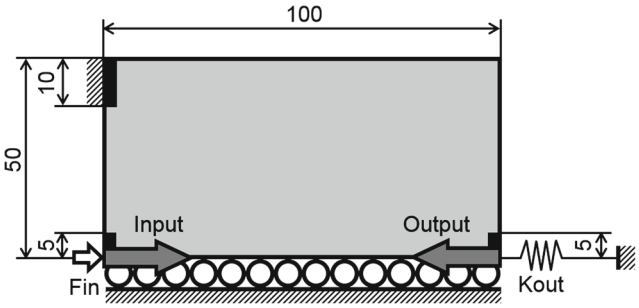

Fig. 3 Design domain and boundary conditions used in the inverter mechanism design. Only half of the domain is used, due to the symmetry. Dimensions in mm

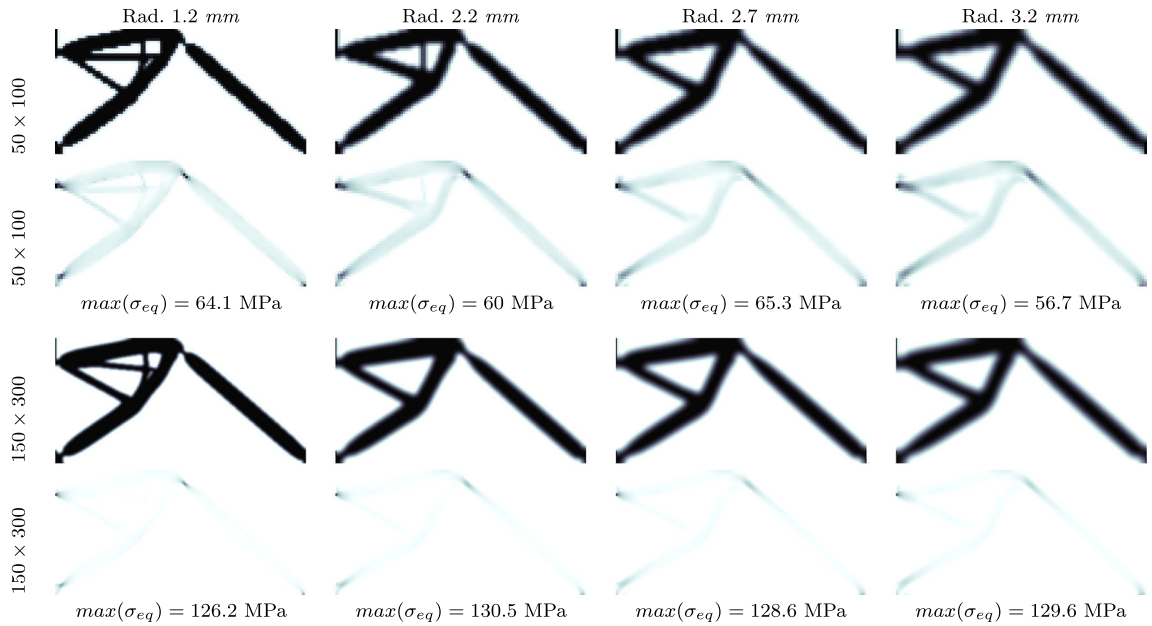

Fig. 4 Topologies and equivalent stress distribution obtained for the inverter mechanism without stress constraint and increasing filtering radius for two different mesh sizes

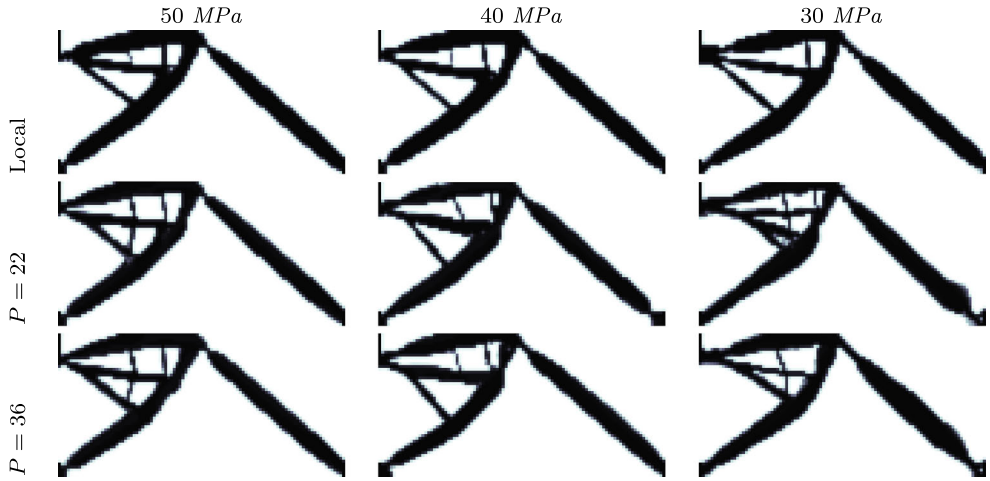

Fig. 5 Topologies obtained for the stress constrained inverter mechanism with the 50 × 100 mesh and 1.2 *mm* filter radius. The first row refers to the local stress constraint approach and the other rows refer to the global stress constraint approach, with different P values

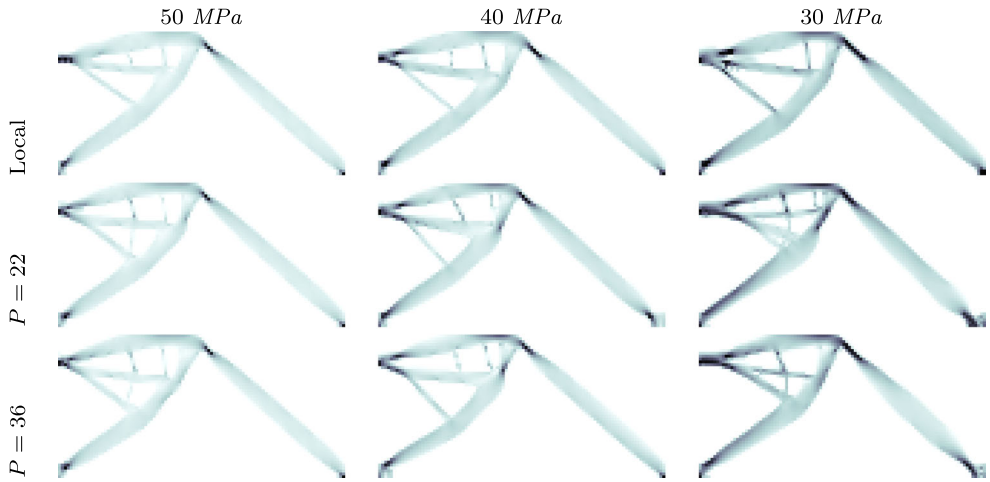

Fig. 6 Stress distribution for the results in Fig. 5

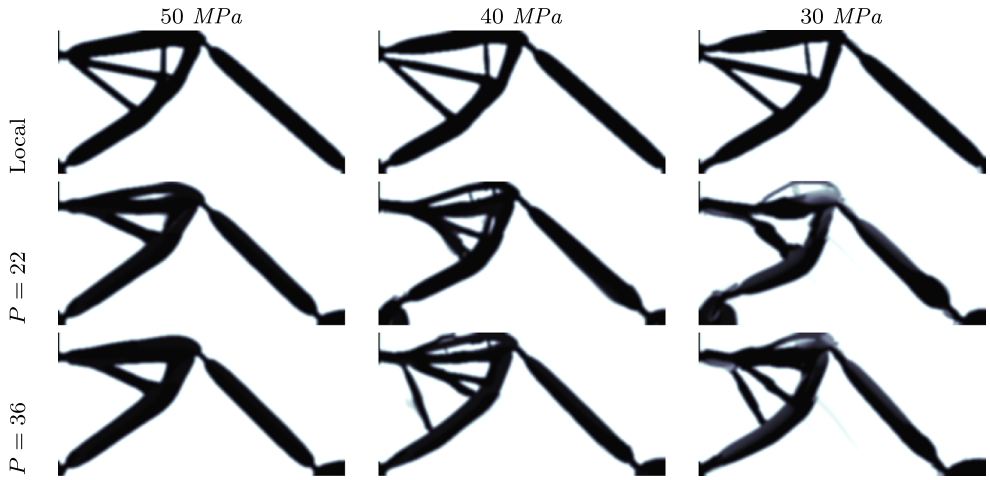

Fig. 7 Topologies obtained for the stress constrained inverter mechanism with 150×300 mesh and 1.2 *mm* filter radius. The first row refers to the local stress constraint approach and the other rows refer to the global stress constraint approach, with different P values

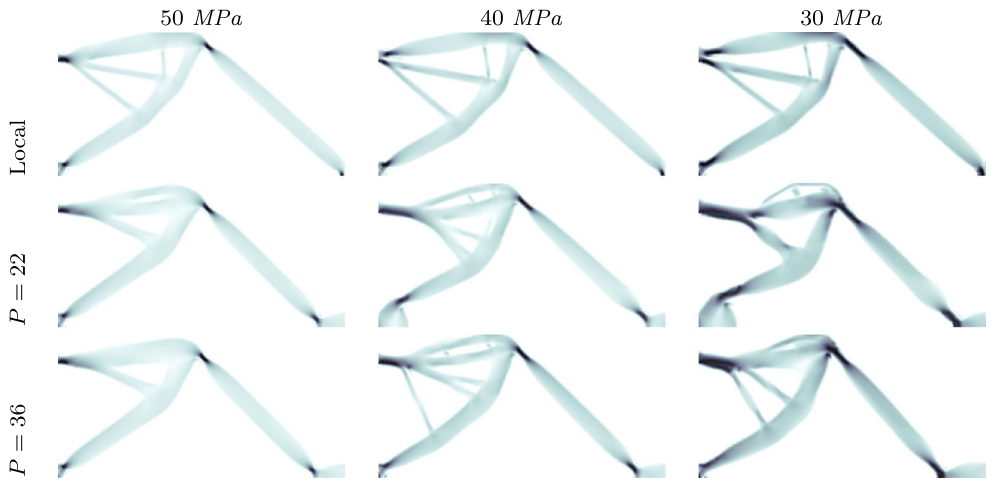

Fig. 8 Stress distribution for the results in Fig. 7

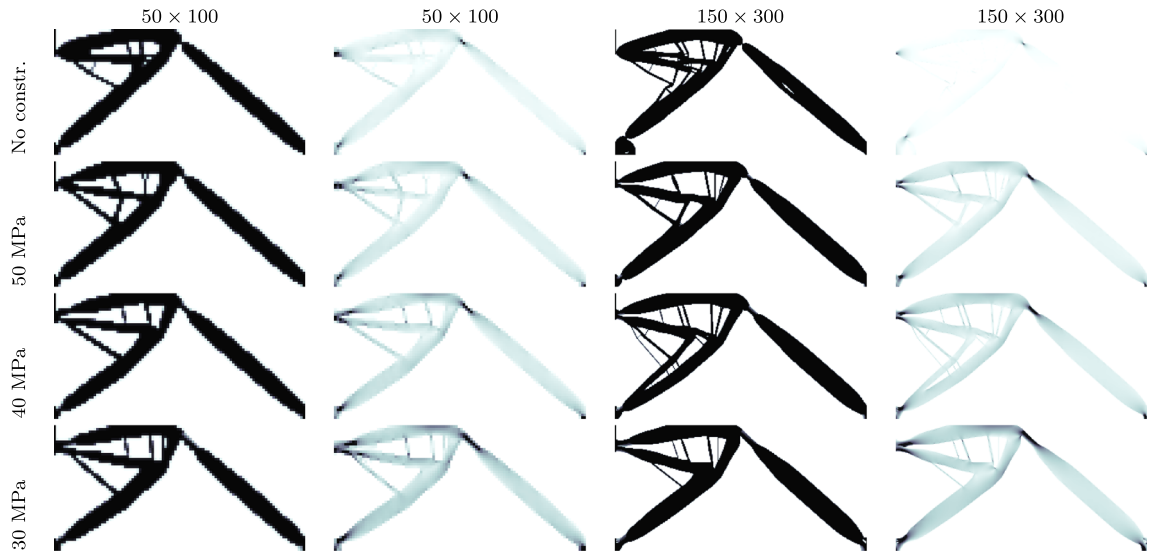

Fig. 9 Topologies and equivalent stress distributions obtained for the local stress constrained inverter mechanism with minimum filtering radius

Table 2 Results summary for the inverter mechanism

	Inverter mechanism	
	Coarse mesh	Fine mesh
Increasing filtering radius only	Hinge free	Hinge free
Local stress constraint + filtering (1.2 *mm*)	Hinge free	Hinge free
Global stress constraint ($P = 22$) + filtering (1.2 *mm*)	Hinge free only for high stress limits	Hinge free only for high stress limits
Global stress constraint ($P = 36$) + filtering (1.2 *mm*)	Hinge free only for high stress limits	Hinge free only for high stress limits
Local stress constraint and minimum filtering radius	Hinge free	Hinge free

length, as well as the input displacement constraint and output displacement used as objective function. Fixed solid elements are imposed in these regions, with one element width.

To evaluate the influence of filter radius and mesh size in eliminating one-node connected hinges for this problem, two different mesh sizes and three different radii are analyzed. Figure 4 shows that, for this problem, it is possible to avoid one-node connected hinges without imposing any stress constraint. Also, it can be seen that as the mesh is refined, there is a clear tendency to concentrate larger stresses in very small regions, indicating that those results can be classified as lumped distributed compliant mechanisms. Those results also show an undesirable effect of using a simple filtering technique, since for a larger radius there are many elements with intermediate relative density along the contour (blurred contour effect). Projection filters may reduce the gray scale at contour when using a large filtering radius (Guest et al. 2004).

For this problem, it is also possible to hinder the appearance of hinges by imposing stress constraint, even without increasing the radius of the filter. Figure 5 shows the effect of both local and global stress constraints for a coarse mesh and 1.2 *mm* radius. Rows with values of P are the results for global stress constraint. Figure 6 shows the equivalent stress distributions associated to the topologies in Fig. 5, where it is clear that the larger stresses occur in the new flexible regions substituting the hinges. Also, the smaller the limit stress, the larger the width of this flexible region, as expected. Thus, for this problem and this mesh size, it is possible to hinder the appearance of hinges and control the width of the compliant link with the local stress constraint and simple filtering.

Table 3 Percentage of the average geometrical advantage for the topologies depicted in Fig. 8

	50 MPa	40 MPa	30 MPa
Local	75.96	75.91	75.32
P = 22	74.04	73,24	68.17
P = 36	74.73	72.41	69.87

The same study is performed with a finer mesh and the same filter radius, as shown in Figs. 7 and 8. The refinement increases the degree of non linearity associated to the global constraint, imposing difficulties to the optimizer. Nonetheless, all the topologies have no hinges and respect the stress limit.

Finally, to test the effectiveness of the local stress constraint in eliminating one-node connections even for the smallest filter radius allowable (just to avoid checkerboard), that is, 10% larger than the element edge size, two mesh sizes and different stress limits are studied. Figure 9 shows both the topologies and equivalent stress distributions. The inverter case studied is a particular case where the local stress constraint alone can hinder the appearance of one-node hinges.

Table 2 shows the summary of all previous results for the inverter compliant mechanism. The strategies of increasing filtering radius and applying local stress constraint were able to achieve hinge-free geometries. The global stress constrained problems did not result in well defined geometries when the stress limits are low, although hinge-free topologies were achieved for higher stress limits. This seems to be a particularity of the optimization algorithm used.

The average geometrical advantage (ratio between the average output and the average input displacements) is used

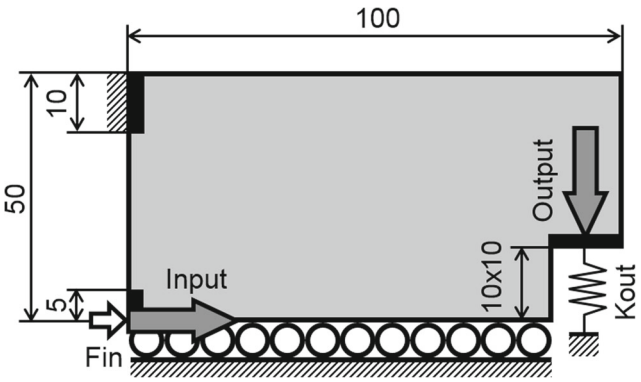

Fig. 10 Design domain and boundary conditions used in the gripper mechanism design. Only half of the domain is used, due to the symmetry. Dimensions in *mm*

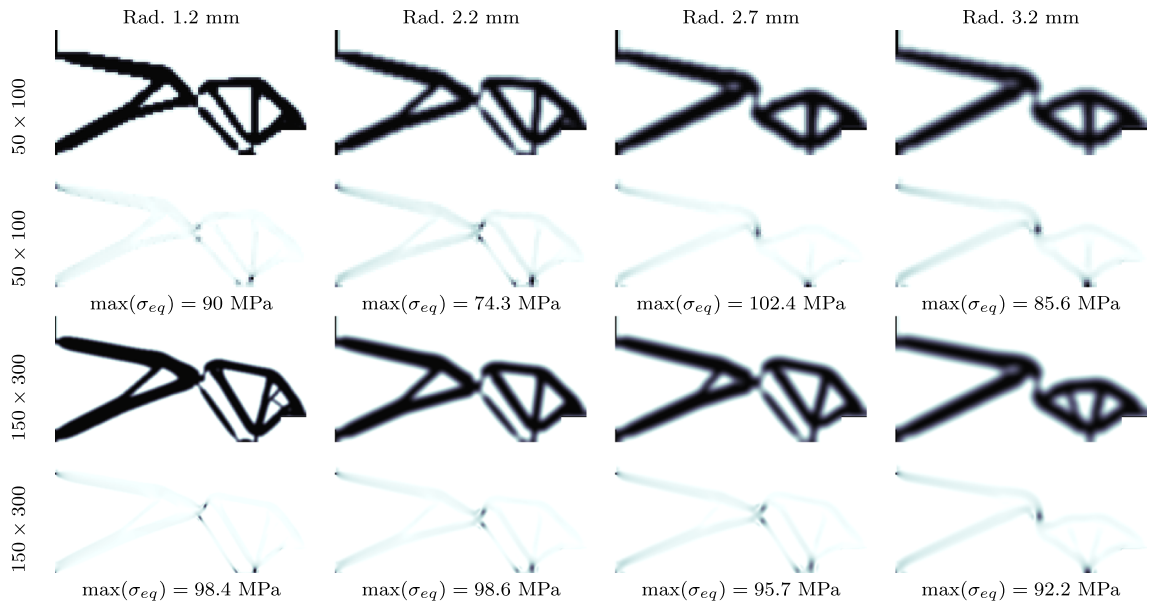

Fig. 11 Topologies and equivalent stress distributions obtained for the gripper mechanism without stress constraint and increasing filtering radius for different mesh sizes

to asses the effectiveness of each solution and to compare the kinematic behavior of the different stress constraints. The average values are used since there are more than one input and output ports. Table 3 show the results obtained for the topologies depicted in Fig. 8. From these results, it can be stated that the local stress constraint has a slightly better kinematic performance when compared to the global approach, for the data set studied in this work. Also, there is a decrease in the geometrical advantage as the stress limit is decreased, as expected.

6.2 Gripper mechanism

Consider the design domain shown in Fig. 10. The gripper mechanism transforms an input in the horizontal direction to an output in the vertical direction. All the optimization parameters are the same as used in inverter compliant mechanism problems.

Figure 11 shows relative densities and stress distribution obtained by varying mesh size and increasing filtering radius, without stress constraint. As it can be seen in this figure, only the combination of a fine mesh plus a large radius was able to provide a thicker connection, although blurred.

Figures 12 and 13 show the topologies and equivalent stress distributions obtained with different stress constraints for the coarse mesh and 1,2 *mm* radius. Different than the inverter case, the use of stress constraint alone does not seem to hinder the appearance of hinges. The same situation is analyzed for a finer mesh and the same filter

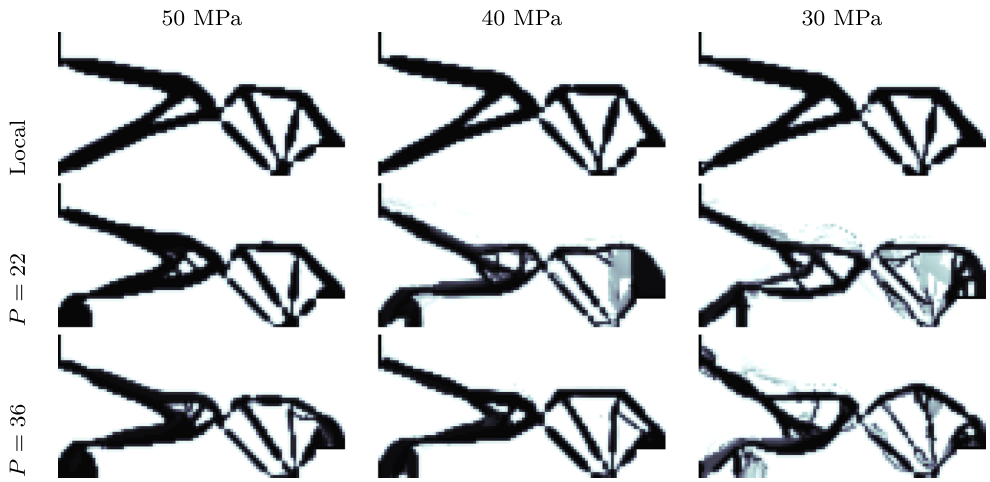

Fig. 12 Topologies obtained for the stress constrained gripper mechanism with the 50 × 100 mesh and 1.2 *mm* filter radius. The first row refers to the local stress constraint approach and the other rows refer to the global stress constraint approach, with different norm values (P)

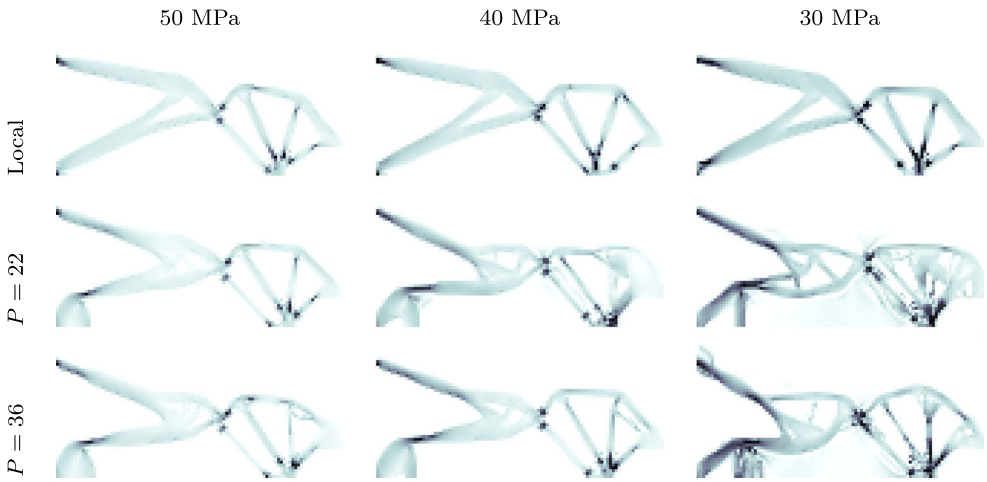

Fig. 13 Stress distribution for the results in Fig. 12

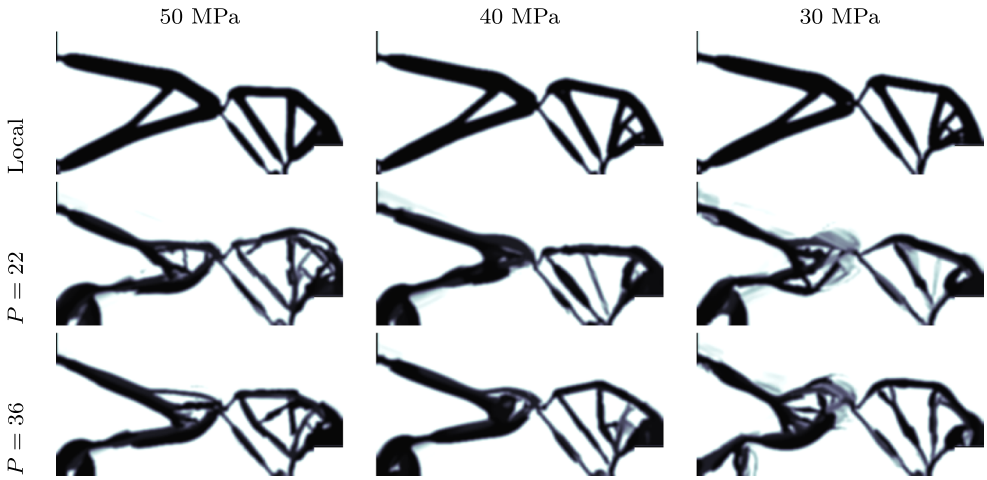

Fig. 14 Topologies obtained for the stress constrained gripper mechanism with the 150×300 mesh and 1.2 *mm* filter radius. The first row refers to the local stress constraint approach and the other rows refer to the global stress constraint approach, with different norm values (P)

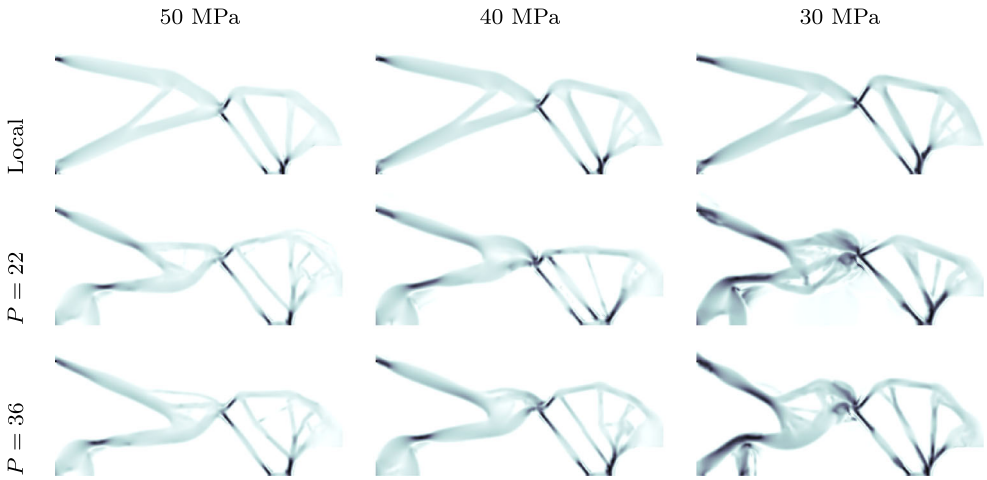

Fig. 15 Stress distribution for the results in Fig. 14

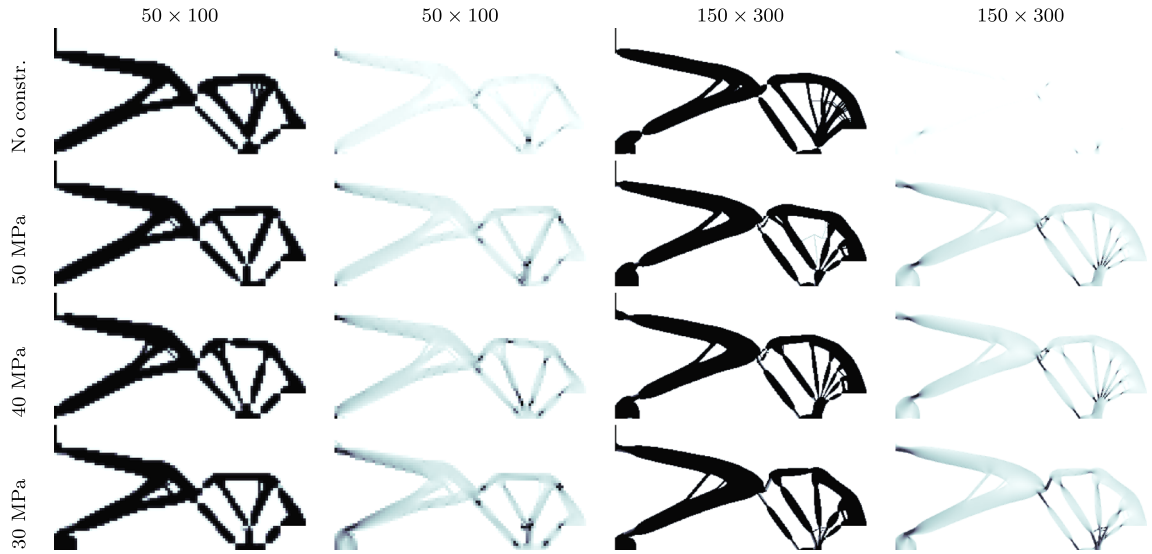

Fig. 16 Topologies and equivalent stress distributions obtained for the local stress constrained gripper mechanism with minimum filtering radius

radius, as shown in Figs. 14 and 15. The results obtained with the local approach show very thin connections and, for the smaller stress limit, can be considered a satisfactory solution.

Again, to test the effectiveness of the local stress constraint in eliminating one-node connections even for the smallest filter radius allowable (just to avoid checkerboard), that is, 10% larger than the element edge size, two mesh sizes and different stress limits are studied for the gripper. Figure 16 shows both the topologies and equivalent stress distributions. It can be stated that for the data set used in this work, the gripper is much more challenging than the inverter with respect to eliminating the hinges.

Table 4 shows the summary of the results obtained for the gripper compliant mechanism. Different from the inverter mechanism problem, in this case is very hard to obtain topologies without one-node connected hinges. The best strategy to obtain hinge-free gripper mechanisms is to apply local stress constraint using a proper filtering radius. The other studied strategies were not able to achieve hinge-free geometries or resulted in misshaped topologies.

Again, the average geometrical advantage (ratio between the average output and the average input displacements) is used to asses the effectiveness of each solution and to compare the kinematic behavior of the different stress constraints. Table 5 shows the results obtained for the topologies depicted in Fig. 15. From these results, it can be stated that the local stress constraint has a slightly better kinematic performance when compared to the global approach, for the data set studied in this work. Also, there is a decrease in the geometrical advantage as the stress limit is decreased, as expected.

Table 4 Results summary for the gripper mechanism

	Gripper mechanism	
	Coarse mesh	Fine mesh
Increasing filtering radius only	Connections with intermediate relative densities	Connections with intermediate relative densities
Local stress constraint + filtering (1.2 mm)	Hinges	Hinge free
Global stress constraint ($P = 22$) + filtering (1.2 mm)	Hinges	Hinges
Global stress constraint ($P = 36$) + filtering (1.2 mm)	Hinges	Hinges
Local stress constraint and minimum filtering radius	Hinges	Very thin connections

Table 5 Percentage of the average geometrical advantage for the topologies depicted in Fig. 15

	50 MPa	40 MPa	30 MPa
Local	75.74	75.31	73.94
P = 22	69.15	68.99	60.83
P = 36	69.94	69.75	63.27

7 Conclusions

Stress constrained topology optimization is thoughtfully discussed in the literature. However, local stress constrained problems are less common when compared to global strategies, due to difficulties that some traditional optimization techniques face. The use of an Augmented Lagrangian formulation together with Optimality Criteria seems to be very efficient when dealing with high number of constraints. This optimization framework was also used with a global stress constraint approach, although the results indicate the need for a more robust optimization algorithm to cope with the degree of non linearity associated to the P norm. Nonetheless, regardless of the optimizer, the use of a global constraint approach in conjunction with the Augmented Lagrangian technique is not discussed in the literature.

Hinge-free compliant mechanisms can be achieved by many ways as shown in literature. Each strategy studied in this work could achieve hinge-free mechanisms for at least one combination of parameters. The best strategy found to obtain hinge-free compliant mechanisms is the combination of a proper value of radius of filtering, a refined mesh and the consideration of local stress constraint.

Observing that properly modeled one-node connected hinges are regions with high stress, applying stress constraint to the design of compliant mechanisms tends to eliminate the solid hinges, replacing it by a (thin) solid connection. The filter acts as a minimum length control over this thin reinforcements and, as result, the joint use of these techniques can prevent the appearance of one-node hinges.

With the consideration of stress constraints the stress distribution along the final geometry is improved, as well as the reliability of the design. Also, for the data set and optimizer considered in this work, it is observed that the local stress constraint approach present better kinematic behavior (geometrical advantage) when compared to the global constraint approach, specially when considering low stress limits.

Acknowledgements The first author would like to thank Embraco for supporting the development of this work. The authors would like to thank Gustavo Assis da Silva for the invaluable discussions during the development of this research. The authors would also thank the anonymous referees for the invaluable comments during the revision of the original manuscript.

References

Bendsøe MP, Kikuchi N (1988) Generating optimal topologies in structural design using a homogenization method. Comput Meth Appl Mech Eng 71(2):197–224. https://doi.org/10.1016/0045-7825(88)90086-2. http://www.sciencedirect.com/science/article/pii/0045782588900862

Bendsøe MP, Sigmund O (2004) Topology Optimization: Theory, Methods and Applications. Springer

Bruggi M (2008) On an alternative approach to stress constraints relaxation in topology optimization. Struct Multidiscip Optim 36(2):125–141. https://doi.org/10.1007/s00158-007-0203-6

Bruns TE, Tortorelli DA (2001) Topology optimization of non-linear elastic structures and compliant mechanisms. Comput Meth Appl Mech Eng 190(26):3443–3459. https://doi.org/10.1016/S0045-7825(00)00278-4. http://www.sciencedirect.com/science/article/pii/S0045782500002784

Cardoso EL, Fonseca JSOF (2004) Strain energy maximization approach to the design of fully compliant mechanisms using topology optimization. Latin American Journal of Solids and Structures 1(3):263–275

Carstensen JV, Guest JK (2013) Improved Two-Phase Projection Topology Optimization. In: Proceedings of the 10th World Conference on Structural and Multidisciplinary Optimization (WCSMO-10), Orlando (FL), pp 1–8

Chen S, Chen W, Lee S (2010) Level set based robust shape and topology optimization under random field uncertainties. Struct Multidiscip Optim 41(4):507–524. https://doi.org/10.1007/s00158-009-0449-2

Cheng GD, Guo X (1997) ϵ-relaxed approach in structural topology optimization. Structural optimization 13(4):258–266. https://doi.org/10.1007/BF01197454

da Silva G, Cardoso E (2017) Stress-based topology optimization of continuum structures under uncertainties. Comput Methods Appl Mech Eng 313:647–672. https://doi.org/10.1016/j.cma.2016.09.049. http://www.sciencedirect.com/science/article/pii/S0045782516312816

de Leon DM, Alexandersen J, Fonseca JSO, Sigmund O (2015) Stress-constrained topology optimization for compliant mechanism design. Struct Multidiscip Optim 52(5):929–943. https://doi.org/10.1007/s00158-015-1279-z

Duysinx P, Bendsøe MP (1998) Topology optimization of continuum structures with local stress constraints. Int J Numer Methods Eng 43(8):1453–1478. https://doi.org/10.1002/(SICI)1097-0207(19981230)43:8<1453::AID-NME480>3.3.CO;2-U

Emmendoerfer H, Fancello EA (2014) A level set approach for topology optimization with local stress constraints. Int J Numer Methods Eng 99(2):129–156. https://doi.org/10.1002/nme.4676

Fancello EA (2006) Topology optimization for minimum mass design considering local failure constraints and contact boundary conditions. Struct Multidiscip Optim 32(3):229–240. https://doi.org/10.1007/s00158-006-0019-9

Guest JK, Prévost JH, Belytschko T (2004) Achieving minimum length scale in topology optimization using nodal design variables and projection functions. Int J Numer Methods Eng 61(2):238–254. https://doi.org/10.1002/nme.1064

Holmberg E, Torstenfelt B, Klarbring A (2013) Stress constrained topology optimization. Struct Multidiscip Optim 48(1):33–47. https://doi.org/10.1007/s00158-012-0880-7

Kogiso N, AHN W, NISHIWAKI S, IZUI K, YOSHIMURA M (2008) Robust topology optimization for compliant mechanisms considering uncertainty of applied loads. Journal of Advanced Mechanical Design, Systems, and Manufacturing 2(1):96–107. https://doi.org/10.1299/jamdsm.2.96

Lau G, Du H, Lim M (2001) Use of functional specifications as objective functions in topological optimization of compliant mechanism. Comput Methods Appl Mech Eng 190(34):4421–4433. https://doi.org/10.1016/S0045-7825(00)00325-X. http://www.sciencedirect.com/science/article/pii/S004578250000325X

Lazarov BS, Schevenels M, Sigmund O (2011) Robust design of large-displacement compliant mechanisms. Mech Sci 2(2):175–182. https://doi.org/10.5194/ms-2-175-2011. https://www.mech-sci.net/2/175/2011/

Lazarov BS, Schevenels M, Sigmund O (2012) Topology optimization with geometric uncertainties by perturbation techniques. Int J Numer Methods Eng 90(11):1321–1336. https://doi.org/10.1002/nme.3361

Le C, Norato J, Bruns T, Ha C, Tortorelli D (2010) Stress-based topology optimization for continua. Struct Multidiscip Optim 41(4):605–620. https://doi.org/10.1007/s00158-009-0440-y

Lee E, Gea HC (2014) A strain based topology optimization method for compliant mechanism design. Struct Multidiscip Optim 49(2):199–207. https://doi.org/10.1007/s00158-013-0971-0

Li L, Khandelwal K (2015a) Topology optimization of structures with length-scale effects using elasticity with microstructure theory. Comput Struct 157:165–177. https://doi.org/10.1016/j.compstruc.2015.05.026. http://www.sciencedirect.com/science/article/pii/S0045794915001728

Li L, Khandelwal K (2015b) Volume preserving projection filters and continuation methods in topology optimization. Eng Struct 85:144–161. https://doi.org/10.1016/j.engstruct.2014.10.052

Li R, Zhu B (2016) An augmented formulation of distributed compliant mechanism optimization using a level set method. Adv Mech Eng 8(8):1–10

Lieu QX, Lee J (2017) Multiresolution topology optimization using isogeometric analysis. Int J Numer Methods Eng 112(13):2025–2047. https://doi.org/10.1002/nme.5593

Liu L, Xing J, Yang Q, Luo Y (2017) Design of large-displacement compliant mechanisms by topology optimization incorporating modified additive hyperelasticity technique. Math Probl Eng :2017. https://doi.org/10.1155/2017/4679746

Lopes CG, Novotny AA (2016) Topology design of compliant mechanisms with stress constraints based on the topological derivative concept. Struct Multidiscip Optim 54(4):737–746. https://doi.org/10.1007/s00158-016-1436-z

Luo J, Luo Z, Chen S, Tong L, Wang MY (2008) A new level set method for systematic design of hinge-free compliant mechanisms. Comput Meth Appl Mech Eng 198(2):318–331. https://doi.org/10.1016/j.cma.2008.08.003. http://www.sciencedirect.com/science/article/pii/S0045782508002922

Luo Y, Wang M, Kang Z (2013) An enhanced aggregation method for topology optimization with local stress constraints. Comput Methods Appl Mech Eng 254:31–41

Maute K, Frangopol DM (2003) Reliability-based design of mems mechanisms by topology optimization. Comput Struct 81(8):813–824. https://doi.org/10.1016/S0045-7949(03)00008-7. http://www.sciencedirect.com/science/article/pii/S0045794903000087, k.J Bathe 60th Anniversary Issue

Midha A, Norton T, Howell L (1994) On the nomenclature, classification and abstractions of compliant mechanisms. Trans ASME 16:270–279

Oest J, Lund E (2017) Topology optimization with finite-life fatigue constraints. Struct Multidiscip Optim 56(5):1045–1059. https://doi.org/10.1007/s00158-017-1701-9

Pian THH, Wu CC (2005) Hybrid and incompatible finite element methods. CRC Press. https://books.google.com.br/books?id=gSrMBQAAQBAJ

Poulsen TA (2002) A simple scheme to prevent checkerboard patterns and one-node connected hinges in topology optimization. Struct Multidiscip Optim 24(5):396–399. https://doi.org/10.1007/s00158-002-0251-x

Saxena A, Mankame ND (2007) Design for manufacture of optimal compliant topologies with honeycomb continuum representation. In: 2007 IEEE congress on evolutionary computation, pp 2956–2963. https://doi.org/10.1109/CEC.2007.4424848

Sigmund O (1997) On the design of compliant mechanisms using topology optimization. Mech Struct Mach 25(4):493–524. https://doi.org/10.1080/08905459708945415

Sigmund O (2007) Morphology-based black and white filters for topology optimization. Struct Multidiscip Optim 33(4):401–424. https://doi.org/10.1007/s00158-006-0087-x

Sigmund O (2009) Manufacturing tolerant topology optimization. Acta Mech Sinica 25(2):227–239. https://doi.org/10.1007/s10409-009-0240-z

Sigmund O, Maute K (2013) Topology optimization approaches: A comparative review. Struct Multidiscip Optim 48(6):1031–1055. https://doi.org/10.1007/s00158-013-0978-6

Wang F, Lazarov BS, Sigmund O (2011) On projection methods, convergence and robust formulations in topology optimization. Struct Multidiscip Optim 43(6):767–784. https://doi.org/10.1007/s00158-010-0602-y

Wang N, Zhang X (2012) Compliant mechanisms design based on pairs of curves. Science China Technological Sciences 55(8):2099–2106. https://doi.org/10.1007/s11431-012-4849-y

Xia Q, Shi T (2016) Topology optimization of compliant mechanism and its support through a level set method. Comput. Methods Appl. Mech. Eng. 305(Supplement C):359–375. https://doi.org/10.1016/j.cma.2016.03.017. http://www.sciencedirect.com/science/article/pii/S0045782516300998

Yang RJ, Chen CJ (1996) Stress-based topology optimization. Structural Optimization 12(2):98–105. https://doi.org/10.1007/BF01196941

Yin L, Ananthasuresh GK (2003) Design of distributed compliant mechanisms. Mech Based Des Struct Mach 31(2):151–179

Zhou M, Lazarov BS, Wang F, Sigmund O (2015) Minimum length scale in topology optimization by geometric constraints. Comput Meth Appl Mech Eng 293:266–282. https://doi.org/10.1016/j.cma.2015.05.003. http://www.sciencedirect.com/science/article/pii/S0045782515001693

Zhu B, Zhang X, Wang N (2013) Topology optimization of hinge-free compliant mechanisms with multiple outputs using level set method. Struct Multidiscip Optim 47(5):659–672. https://doi.org/10.1007/s00158-012-0841-1

Zhu B, Zhang X, Fatikow S (2014) A multi-objective method of hinge-free compliant mechanism optimization. Struct Multidiscip Optim 49(3):431–440. https://doi.org/10.1007/s00158-013-1003-9